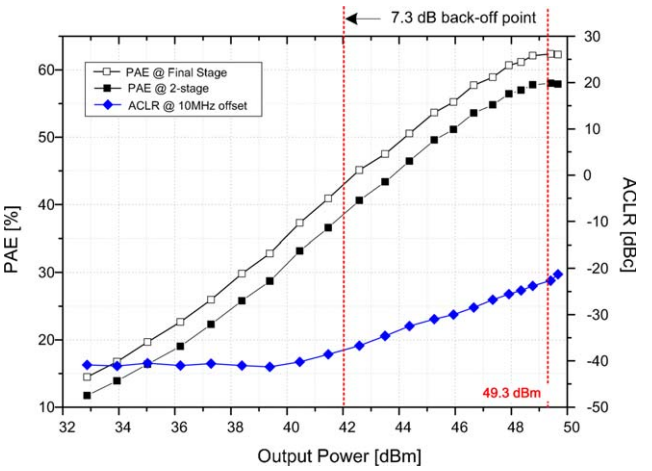

Figure 6 Measured power added efficiency (PAE) and adjacent channel leakage ratio (ACLR) of the proposed amplifier for the LTE test signal. [Color figure can be viewed in the online issue, which is available at wileyonlinelibrary.com]

TABLE 1 Comparison of Doherty Amplifier Characteristics

References	OPBO (dB)	Spec.	PAE (%)	Linearity (dBc)
[5]	7.3	3GPP	30	−25.0
[6]	7.3	3GPP	34	−37.0
[7]	7.3	3GPP2	38.5	−33.0
This work	7.3	3GPP	43.2	−37.2

OPBO, output power back-off; PAE, power added efficiency.

bandwidth. The simulation results of the proposed UDPA with embedded drivers show complete compensation of the maximum output power reduction of the conventional UDPA. The efficiency with the optimized linearity of the proposed UDPA is better than the highest efficiency with similar linearity of the conventional UDPA. At 7.3 dB OPBO for 49.3 dBm output power, the proposed amplifier improved 5.7% power added efficiency (PAE) with comparison of the conventional UDPA efficiency.

Figure 6 shows the measured PAE and IMD for the proposed two-stage amplifier. An efficiency of 40% and an IMD of −43 dBc for the entire circuit were obtained at the output power of 15 W. With efficiency optimization, an efficiency of 43.3% is achieved with an IMD of −37 dBc. The measured results in Figure 6 show that the maximum output power reduction is not completely compensated due to the limitation of the fine tuning of the bias control and the output impedance during the measurement.

Figure 7 shows the measured PAE and adjacent channel leakage ratio (ACLR) of the amplifier for the LTE test. A PAE of 43% and IMD of −37 dBc at the 10 MHz offset frequency were obtained, respectively.

Table 1 shows the performance comparison between the proposed two-stage UDPA and the published Doherty PA at 7.3 dB OPBO. The proposed two-stage UDPA achieved more improved efficiency and linearity compared with the previous works even though the proposed amplifier has a simpler structure.

4. CONCLUSION

A highly efficient UDPA using an embedded drive amplifier was designed and fabricated for LTE test signal. The proposed amplifier can extend the turn on point by the peak to average ratio of the input signal and achieve maximum output power by optimizing two gate biases in the two-stage peaking amplifier.

ACKNOWLEDGMENT

The present research has been conducted by the Research Grant of Kwangwoon University in 2013.

REFERENCES

1. J.Y. Lee, J.Y. Kim, J.H. Kim, K.J. Cho, and S.P. Stapleton, A high power asymmetric Doherty amplifier with improved linear dynamic range, IEEE MTT-S International Microwave Symposium Digest, Vol. 3, San Francisco, CA, 2006, 1348–1350.
2. K.J. Cho, W.J. Kim, S.P. Stapleton, J.H. Kim, B. Lee, J.J. Choi, J.Y. Kim, and J.C. Lee, Design of N-way distributed Doherty amplifier for WCDMA and OFDM applications, IEEE Electron Lett 43 (2007), 577–578.
3. D.H. Jang, J.Y. Kim, and J.H. Kim, 46W high efficiency unbalanced Doherty power amplifier in extended output power back-off, Microwave Opt Technol Lett 54 (2012), 1612–1614.
4. S. Bousnina and M. Ghannouchi, Analysis and experimental study of an L-band new topology Doherty amplifier, IEEE MTT-S International Microwave Symposium Digest, Phoenix, AZ, 2001, 935–938.
5. J.G. Ghim, K.J. Cho, J.H. Kim, and S.P. Stapleton, A high gain Doherty amplifier using embedded drivers, IEEE MTT-S International Microwave Symposium Digest, Vol. 3, San Francisco, CA, 2006, 1838–1841.
6. Y. Lee, M. Lee, S. Kam, and Y. Jeong, A highly linear and efficient three-way Doherty amplifier using two-stage GaN HEMT cells for repeater systems, Microwave Opt Technol Lett 51 (2009), 2895–2898.
7. S.H. Sang, D.H. Jang, J.Y. Kim, and J.H. Kim, Inverted asymmetric Doherty power amplifier driven by two-stage symmetric Doherty amplifier, IEEE Electron Lett 46 (2010), 1208–1209.

ARTIFICIAL NEURAL NETWORKS FOR THE CHROMATIC DISPERSION PREDICTION OF PHOTONIC CRYSTAL FIBERS

V. F. Rodríguez-Esquerre,[1] J. J. Isídio-Lima,[1] A. Dourado-Sisnando,[1] and F. G. Simões Silva[1,2]
[1] Department of Electrical Engineering, Federal University of Bahia, UFBA, Bahia, Brazil; Corresponding author: anderson.sisnando@ufba.br
[2] IFBA, Brazil

Received 16 January 2013

ABSTRACT: *Multilayer perceptron artificial neural networks have been used for the efficient evaluation and prediction of the chromatic dispersion properties of microstructured optical fibers, with very low computational resources and efforts in an easy, efficient, and simple way.* © 2013 Wiley Periodicals, Inc. Microwave Opt Technol Lett 55:2179–2181, 2013; View this article online at wileyonlinelibrary.com. DOI 10.1002/mop.27753

Key words: *ANNs; chromatic dispersion; microstructured fibers*

1. INTRODUCTION

Photonic crystal fibers (PCFs) also known as microstructured optical fibers, are currently under exhaustive study because several devices for optical processing of light can be designed and also due to their flexibility and the feasibility for tailoring their main properties (chromatic dispersion, modal area, single-mode operation, etc.,) by adjusting their optical and geometrical parameters in a judicious way [1–7]. They are classified in two categories according to their guiding mechanism: The holey fiber and the

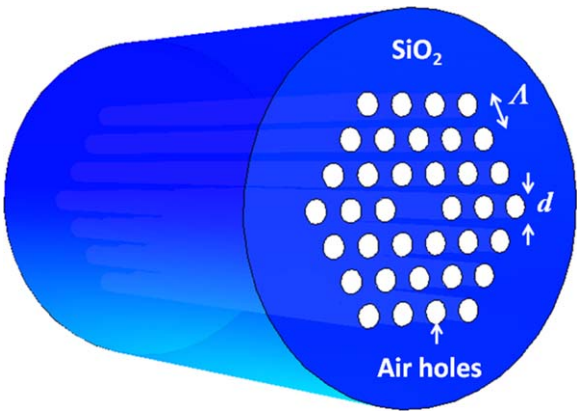

Figure 1 Schematic of the index-guiding microstructured optical fiber. [Color figure can be viewed in the online issue, which is available at wileyonlinelibrary.com]

index-guiding fiber, where the guiding mechanism is the photonic band gap and the total internal reflection, for the former and the later, respectively. In this work, the index-guiding fiber has been considered to be analyzed and their chromatic dispersion has been chosen as the parameter to be predicted by multilayer perceptron (MLPs) artificial neural networks (ANNs). See Figure 1.

The chromatic dispersion is one of the most important parameters of optical fibers, and it is directly related with the pulse broadening when the same propagates along the fiber, limiting in most of the cases the maximum distance of an optical link according with $L_{\max} = (4B|D|\Delta\lambda)^{-1}$, where B is the transmission bit rate, D the chromatic dispersion, and $\Delta\lambda$ the linewidth of the optical source.

There are approximate empirical relations to obtain the chromatic dispersion of PCFs [4]. However, numerical techniques, such as the finite element method, are the most appropriated approaches for this analysis. They are in general the most used for the modeling of such structures, although the same requires a deep knowledge of advanced electromagnetic theory and also great computational efforts and resources. In order to obtain the chromatic dispersion by using numerical techniques, first, the geometry of the optical fiber under analysis should be discretized and all the information about the same is used to assemble an eigenvalues matrix system, then the effective refractive index, n_{eff}, must be obtained with a high accuracy at several wavelengths since a second derivative of n_{eff} is needed for the chromatic dispersion computation, given by $D = -(\lambda/c)\left(\partial^2 n_{eff}/\partial\lambda^2\right)$, where λ and c are the operating wavelength and the speed of light in the free space, respectively. In such approach, the material dispersion is already included. Consequently, numerical methods are in general time consuming.

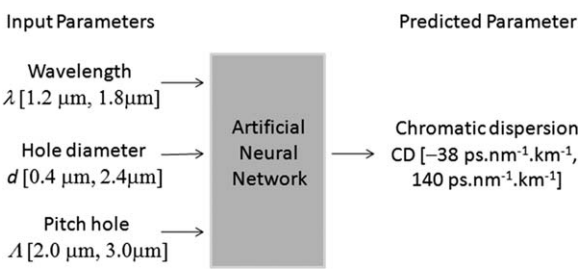

Figure 2 Input and output parameters of the ANN model used to predict the chromatic dispersion of microstructured optical fibers

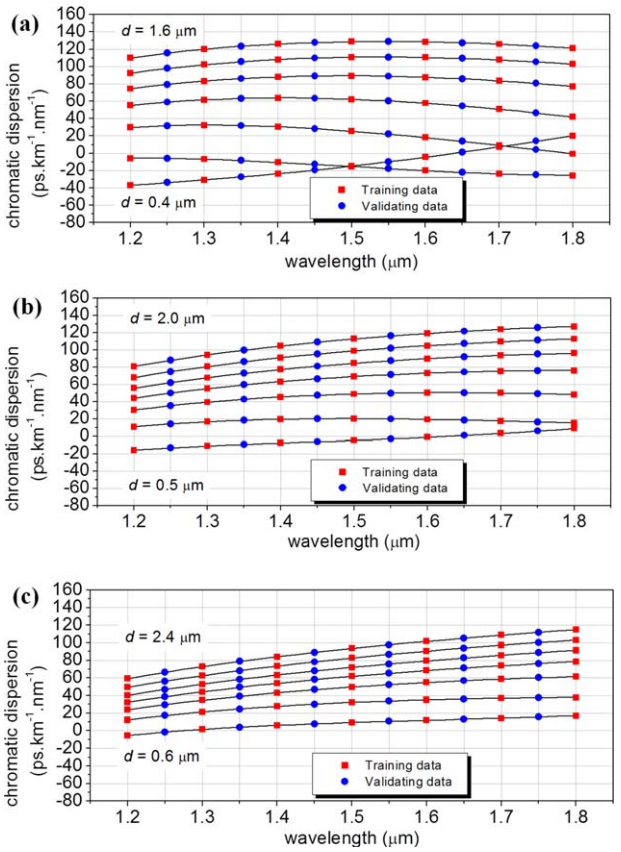

Figure 3 Chromatic dispersion obtained by the ANN for the training and validating data set for several pitch hole (a) $\Lambda = 2$ μm, (b) $\Lambda = 2.5$ μm, and (c) $\Lambda = 3$ μm. The continuous line is related to data from [4]. [Color figure can be viewed in the online issue, which is available at wileyonlinelibrary.com]

On the other hand, ANNs have been used in photonics for the modeling of planar waveguides based couplers and optical fiber based couplers [8] and also for the analysis of PCFs [9,10] and patch antennas [11]. The main advantages of an ANN based models are their simplicity, the reduced time, and computational effort and also its application for synthesis problems. In this work, several neural networks architectures have been implemented for the modeling and the prediction of the chromatic dispersion of several geometrical configurations of PCFs as shown in Figure 1. For this purpose, previously published data have been used in order to train the ANN [4]. The best ANN configuration has been used to compare our results with the previously ones published [4] and finally maps of chromatic dispersion have been generated by using the ANN model.

In order to show the validity and usefulness of the application of neural networks, the prediction of the chromatic dispersion of a PCF is presented.

2. THE NEURAL NETWORK

The neural network used here was the MLP with two hidden layers because they are simple, exhibit a quick convergence and a high efficiency during the ANN training process. Several configurations have been tested in this research and the best configuration was obtained by using 7 and 23 neurons in the hidden layers. The activating functions in all cases were the tangent hyperbolic for the hidden layers and the linear one at the output layer, respectively. The training process was carried out with the Levenberg-Maquardt algorithm. The input variables considered

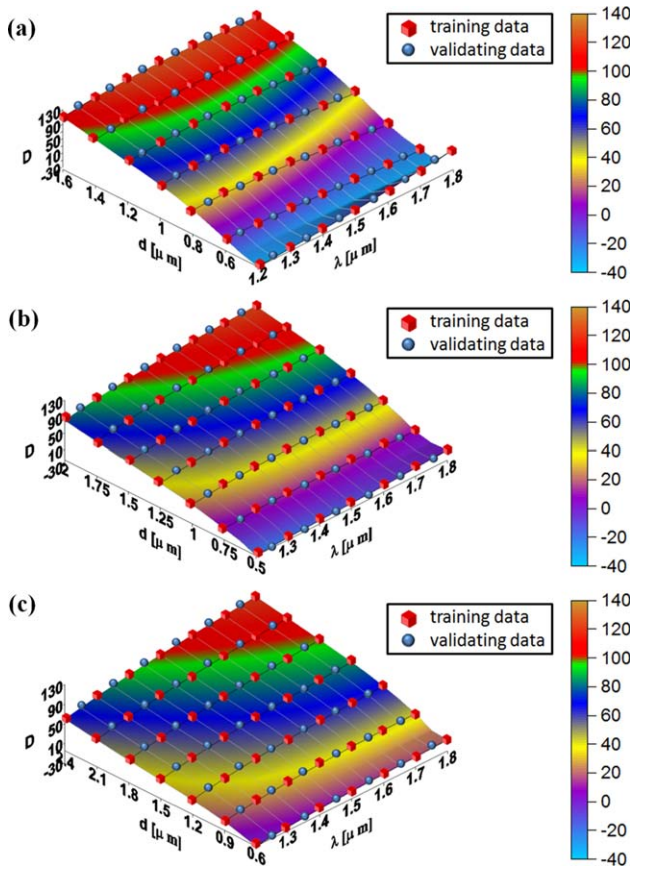

Figure 4 Chromatic dispersion maps for pitch hole values of (a) $\Lambda = 2$ μm, (b) $\Lambda = 2.5$ μm, and (c) $\Lambda = 3$ μm. [Color figure can be viewed in the online issue, which is available at wileyonlinelibrary.com]

in this work are the operating wavelength, the pitch hole, and the hole diameter. The output or predicted variable was the chromatic dispersion, see Figure 2. The training data set has been obtained from [4].

3. NUMERICAL RESULTS

In order to validate the proposed neural network approach, the microstructured index-guiding fiber, shown in Figure 1, has been considered for analysis and its chromatic dispersion has been computed for several parameter values. The PCF is composed by fused silica (SiO2) with several concentrically disposed rings of air holes in a hexagonal lattice. The chromatic dispersion necessary for training the neural network has been obtained from [4], where the material dispersion has been already taken into account in the calculations by using the Sellmeier equations at room temperature ($T = 300$ K). The training data used for each variable shown in Figure 1(a) are restricted to the intervals: λ [1.2 μm, 1.8 μm] (in order to cover the entire communication window); Λ [2 μm, 3 μm]; d [0.4 μm, 2.4 μm]. As a result, the chromatic dispersion lies in the interval CD [-38, 140 ps nm^{-1} km^{-1}]. A set of 147 samples have been used for neural network training. An additional set of 126 samples were separated in order to test the neural network architecture with the best behavior.

The neural networks were configured to run 10,000 epoch, the learning rate was 0.005 and for the best ANN, the results have converged after 6432 epoch taking 210 sec. The quadratic error at the end of the training was 8×10^{-5}. The neural network results are plot together to the data obtained from [4] in Figure 3. The red squares and blue dots correspond to the training and validating data, respectively, and the solid lines correspond to the data available in [4]. It can be seen an excellent agreement between ANN data and the ones previously published in [4]. It can be observed a nonlinear behavior of the chromatic dispersion and the PCF parameters. The error between the values given in [4] and the ANN based model obtained here, are less than 1 ps nm^{-1} km^{-1}.

Once the ANN has been validated, it has been used to generate a map of the chromatic dispersion by scanning the parameters values in the entire interval. The results can be seen in Figures 4(a)–4(c) where the training and validated data, represented by red cubes and blue spheres, respectively, have been also put together. It can be observed a nonlinear relation of the chromatic dispersion and the optical/geometrical parameters. It makes the ANN a suitable tool for this problem. The error between the published results [4] and the ANN ones are less than 2 ps nm^{-1}.km^{-1} in the entire interval.

A Laptop with Intel Pentium Processor T3400, 2.16 GHz of clock and 2 Gb of RAM running on Windows Vista Starter has been used in all simulations.

4. CONCLUSION

In conclusion, the chromatic dispersion of an index guiding microstructured fiber has been efficiently computed by using a relatively effortless neural network algorithm. The model obtained is very simple, accurate and it is less time consuming as well it requires less computational effort than classical numerical techniques used for the analysis of this kind of problems.

ACKNOWLEDGMENT

This work was supported by INCT/CNPq Fotonicom, UFBA, IFBA, CNPq Process 302390/2009-0, FAPESB and CAPES.

REFERENCES

1. P. St. J. Russell, Photonic crystal fibers, Science 299 (2003), 358–362.
2. J.C. Knight, Photonic crystal fibres, Nature 424 (2003), 847–851.
3. J.C. Knight, J. Broeng, T.A. Birks, and P.St.J. Russell, Photonic band gap guidance in optical fibers, Science 282 (1998), 1476–1478.
4. K. Saitoh and M. Koshiba, Empirical relations for simple design of photonic crystal fibers, Opt Express 13 (2005), 267–274.
5. K. Saitoh and M. Koshiba, Numerical modeling of photonic crystal fibers, J Lightwave Technol 23 (2005), 3580–3580.
6. A. Martinez and J. Bravo-Abad, Wavelength demultiplexing structure based on coupled-cavity waveguides in photonic crystals, Fiber Integrated Opt 22 (2010), 151–160.
7. V. Pureur, A. Bétoumé, G. Bouwmans, L. Bigot, A. Kudlinsky, K. Delplace, A. Le Rouge, Y. Quiquempois, and M. Douay, Overview on solid core photonic bandgap fibers, Fiber Integrated Opt 28 (2009), 27–50.
8. V.F. Rodríguez-Esquerre, A. Dourado-Sisnando, and F.G.S. Silva, Neural network analysis and design of directional couplers, Paper no. JTuB25. Proceeding of the Integrated Photonics Research, Silicon and Nanophotonics (IPRSN), pp. 1–3.
9. J. Li and Z. Bao, Neural network model of optical fiber direction coupler design, Proceeding of the Optical Modeling and Performance Predictions, SPIE 5178, 2004, pp. 238–245.
10. M.F.O. Hameed, S.S.A. Obayya, K. Al-Begain, A.M. Nasr, and M.I. Abo el Maaty, Accurate radial basis function based neural network approach for analysis of photonic crystal fibers, Opt Quantum Electron 40 (2008), 891–905.
11. A. Ouchar, R. Aksas, and H. Baudrand, Artificial neural network for computing the resonant frequency of circular patch antennas, Microwave Opt Technol Lett 47 (2005), 564–566.